SYNTHESIS OF REDUCED GRAPHENE OXIDE LOADED-ZnS/Ag₂S QUANTUM DOT HETEROSTRUCTURES VIA ION EXCHANGE FOR HIGH-EFFICIENCY PHOTOCATALYTIC HYDROGEN PRODUCTION

B. ZENG[a,b*], W. ZENG[a]
ᵃHunan Collaborative innovation Center for construction and development of Dongting Lake Ecological Economic Zone, Changde 415000, People's Republic of China
ᵇCollege of Mechanical Engineering, Hunan University of Arts and Science, Changde 415000, People's Republic of China

Efficient photocatalytic systems are needed to convert solar energy into chemical energy. In this work, a novel visible light-driven photocatalyst based on graphene loaded-ZnS/Ag₂S quantum dots was prepared through a cation-exchange reaction between ZnS quantum dots and AgNO₃. The resulting photocatalyst exhibited a high visible-light photocatalytic activity for H₂ production because of photoinduced interfacial charge transfer (IFCT) in the ZnS/Ag₂S quantum dot heterostructures and electron transfer from ZnS/Ag₂S to graphene. This work broadens the scope of designs for high-efficiency transition metal/sulfide photocatalysts.

1. Introduction

In recent decades, the production of hydrogen via photocatalytic water splitting using solar energy has attracted much attention because of its promise as a strategy to solve environmental and energy problems [1]. Because of its very negative reduction potential, ability to rapidly generate electron-hole pairs, environmental compatibility, and low cost, zinc sulfide (ZnS) has emerged as an important semiconductor photocatalyst [2]. However, ZnS has a wide band gap and is only responsive to ultraviolet (UV) light, which accounts for only a small fraction of the solar spectrum. Therefore, photocatalysts are needed for splitting water that are capable utilizing a broader range of visible light [3].

ZnS has been combined with narrow band gap semiconductors to improve visible-light driven photocatalysis [4]. Silver sulfide (Ag₂S), which has a band gap of 1.0 eV, can narrow the band gap of ZnS and improve its visible-light activity [5]. ZnS/Ag₂S nanoparticles have been prepared that are hundreds of nanometers in diameter. For example, Zhang et al. fabricated ZnS/Ag₂S nanospheres with average diameters of approximately 350 nm, and these materials were used to degrade about 96% of methyl orange (MO) within 15 min [6]. Reddy et al. synthesized graphene oxide-coated ZnS-Ag₂S ternary composites with diameters between 0.5 μm and 2 μm. The composite had a better degradation rate (54.08%) than bare ZnS and Ag₂S under illumination by sun light [7]. However, the use of nanocomposites is very limited by their low efficiencies, especially as solar photocatalysis.

Reducing particle size is known to increase specific surface area and can thereby increase the number of reactive sites [8]. Because of their large surface-to-volume ratios, quantum dots are excellent light-harvesting photosensitizers. More importantly, the photovoltaic properties of quantum dots, including their abilities to effectively capture photons, generate electron-hole pairs,
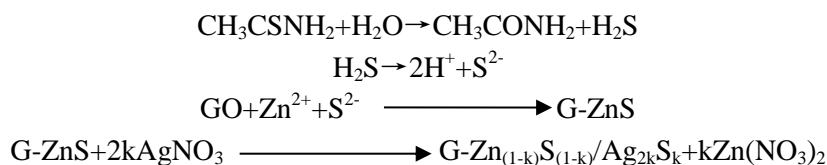
---

and separate electrons and holes at interfaces, are favorable for enhancing photochemical activity [9-10].

To further optimize catalytic performances, appropriate nanostructures can be created in hybrid materials containing quantum dots and carbon. The high electrical conductivity and layered structure of graphene make it an excellent electron-transport matrix [11]. Recently, graphene-quantum dot composites have become a popular topic of research [12]. However, to the best of our knowledge, little work has been done on graphene-ZnS/Ag$_2$S quantum dot heterostructure composites.

In this work, we synthesized a nanocomposite of ZnS/Ag$_2$S quantum dot heterostructures decorated with graphene (G-ZnS/Ag$_2$S QD) using a cation-exchange method. The activity for visible light-driven photocatalytic H$_2$ production was investigated, and a mechanism for charge transfer was proposed.

2. Experimental details

In a typical synthesis, 3 mL of 1 g L^{-1} graphene oxide (GO) and 250 mL of 2 g L^{-1} Zn(AC)$_2$·2H$_2$O were ultrasonicated to form a homogeneous mixture. To this mixture, 100 mL of 2 g L^{-1} thioacetamide (TAA) was added. The blended mixture was heated for 30 min in a microwave, and a gray precipitate was obtained. The precipitate was washed in deionized water several times in order to remove TAA residue. The washed product was added to a 0.15 g L^{-1} AgNO$_3$ aqueous solution to undergo an ion-exchange reaction in a microwave for 30 min. The series of samples prepared at nominal Ag$^+$/Zn^{2+} molar ratios of x = 1, 2, and 3 are labeled as G-ZnS/Ag$_2$S-x QD. For comparison, ZnS and graphene-ZnS quantum dots (G-ZnS QD) were also prepared using a similar procedure.

$$CH_3CSNH_2 + H_2O \rightarrow CH_3CONH_2 + H_2S$$
$$H_2S \rightarrow 2H^+ + S^{2-}$$
$$GO + Zn^{2+} + S^{2-} \longrightarrow G\text{-}ZnS$$
$$G\text{-}ZnS + 2kAgNO_3 \longrightarrow G\text{-}Zn_{(1-k)}S_{(1-k)}/Ag_{2k}S_k + kZn(NO_3)_2$$

Characterization. Sample morphology and structure were characterized by X-ray diffraction (XRD, D5000), scanning electron microscopy (SEM, S4800), and transmission electron microscopy (TEM, JEM-2100F). Raman spectra were obtained using a JY Horiba T64000 Raman spectrometer. Fourier transform infrared spectroscopy (FTIR) was performed using a Perkin Elmer FTIR spectrometer. Elemental analysis was performed with X-ray photoelectron spectroscopy (XPS, K-Alpha 1063), photoluminescence (PL) measurements (Hitachi F-7000).

Photocatalytic H$_2$ production. Photocatalytic H$_2$ production was carried out with a Labsolar-III AG system (Beijing Perfectlight Technology Co., Ltd.) using a 300 W xenon lamp as a light source. Photocatalyst (50 mg) containing 0.1 M Na$_2$S and 0.05 M Na$_2$SO$_3$ as sacrificial reagents was dispersed in 80 mL of aqueous solution. Before irradiation, the sealed reactor was purged with nitrogen for 30 min to remove air. Throughout the experiment, the photocatalyst particles were suspended by continuous stirring. Hydrogen was measured using gas chromatography (Labthink GC-7800).

3. Results and discussion

The XRD patterns of the samples are shown in Fig. 1a. The XRD pattern of bare ZnS contained typical diffraction peaks at 28.64°, 47.75°, and 56.53°, which corresponded to the (111), (110), and (112) planes of ZnS (JPCDS 36-1450), respectively. The XRD pattern of the G-ZnS

QD composite was similar to that of pure ZnS, and no characteristic peaks for graphene were observed, possibly because a low concentration of graphene was added. For the G-ZnS/Ag$_2$S-2 QD, new diffraction peaks at 34.2° were ascribed to the (-121) crystal planes of Ag$_2$S (JCPDS No. 14-0072). These results indicate that ZnS, Ag$_2$S, and graphene were successfully formed.
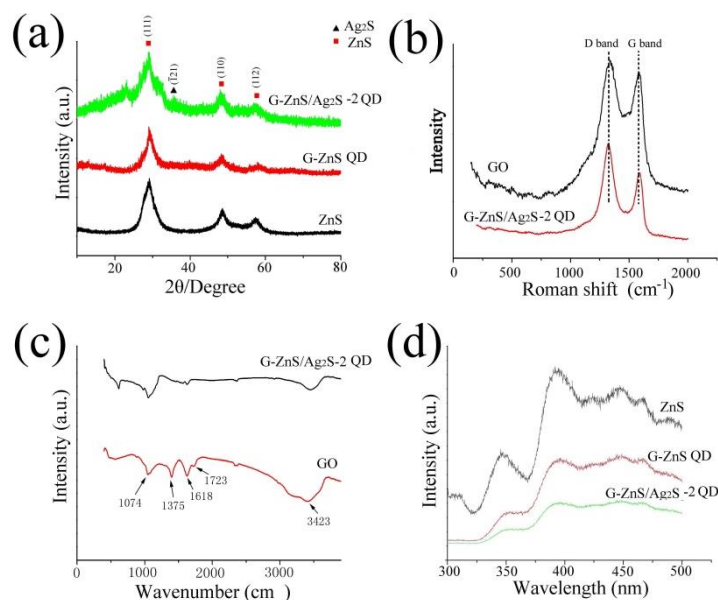

Fig. 1.(a) XRD, (b) Raman spectra, (c)FTIR spectra, (d) PL spectra of the samples

Typical Raman spectra of the GO and G-ZnS/Ag$_2$S-2 QD samples are shown in Fig. 1b. GO exhibited a D band at 1323 cm^{-1}, arising from sp3 defects such as topological defects, vacancies, and dangling bonds. GO also exhibited a G band at 1592 cm^{-1}, which resulted from sp2 hybridized C atoms on graphene's basal plane. For G-ZnS/Ag$_2$S-2 QD, these two peaks were in the same position. However, the intensity ratio of the D and G peaks (I$_D$/I$_G$) of G-ZnS/Ag$_2$S-2 QD (0.92) was higher than that of GO (0.81), indicating the presence of more sp3 defects in carbon. These defects were attributed to strongly coupled interactions between graphene and the metallic nanoparticles [13]. This allowed for the effective transfer and separation of photogenerated electron-hole pairs.

Fig. 1c shows the FTIR spectra of GO and G-ZnS/Ag$_2$S-2 QD. For pure GO, typical peaks for GO were observed, including alkoxy C–O stretching (1074 cm^{-1}), carboxyl O–H stretching (1375 cm^{-1}), the C=O stretching vibrations of carboxyl or carbonyl groups (1723 cm^{-1}), the –O–H bending of adsorbed H$_2$O molecules (1618 cm^{-1}), and the H–O stretching vibrations of surface hydroxyl groups (3403 cm^{-1}). In G-CuS/Ag$_2$S-2 QD, the intensity of these characteristic absorption bands decreased or disappeared in some cases, indicating a significant reduction in the amount of GO. This reduction of GO, which has an excellent electrical conductivity, guaranteed efficient electron transport and promoted improved photocatalytic efficiency [14].

Fig. 1d shows PL spectra for the samples at 280 nm. ZnS emitted strong PL signals with peaks at 346 nm, 398 nm, 446 nm, 467 nm, and 460 nm. Clearly, the PL emission at these characteristic wavelengths was quenched in G-ZnS QD compared with the signal observed for pure ZnS. This indicated that electron transfer from ZnS to graphene was improved. When heteronanostructures formed in the G-ZnS/Ag$_2$S QD nanocomposites, the PL emission intensities decreased further, indicating a much lower recombination rate for photoinduced electrons and holes. These results revealed that both the graphene and heteronanostructures promoted photoinduced charge separation in the nanocomposite [15].
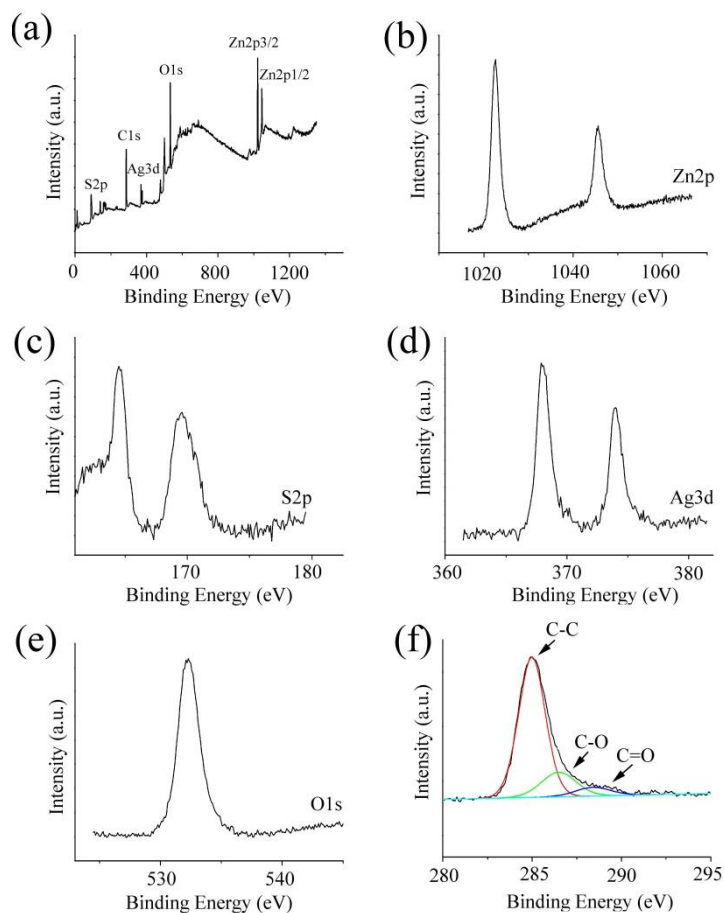
Fig. 2. Typical XPS spectra of the G-ZnS/Ag₂S QD-2: (a) survey spectra, (b) Typical Zn2p region, (c) Typical S2p region, (d) Typical Ag3d region, (e) Typical O1s region, (f) Typical C region

XPS was used to confirm the chemical states of the Zn, S, Ag, O, and C atoms in the G-ZnS/Ag₂S-2 QD nanocomposites. Full XPS survey spectra revealed that Zn, Ag, S, and C were the most prominent elements in the samples. High-resolution Zn 2p XPS spectra are shown in Fig. 2b. The two peaks at binding energies of 1022.48 eV and 1045.58 eV were assigned to Zn 2p3/2 and Zn 2p1/2, respectively. Fig. 2c,d shows peaks for S (S 2p1/2 at 164.48 eV; S 2p3/2 at 169.58 eV) and Ag (Ag 3d5/2 at 367.88 eV; Ag 3d3/2 at 373.98 eV), respectively. The peak at 532.58 eV was assigned to Ag–O–C bonds (Fig. 2e). Fig. 2f shows the C 1s XPS spectra of the nanocomposites. The amount of oxygenated functional groups (286.43 eV for C–O and 288.56 eV for O–C=O) in the nanocomposites was drastically decreased. The dominance of the C=C–C peak was believed to indicate efficient electron transport in the nanocomposites [16].
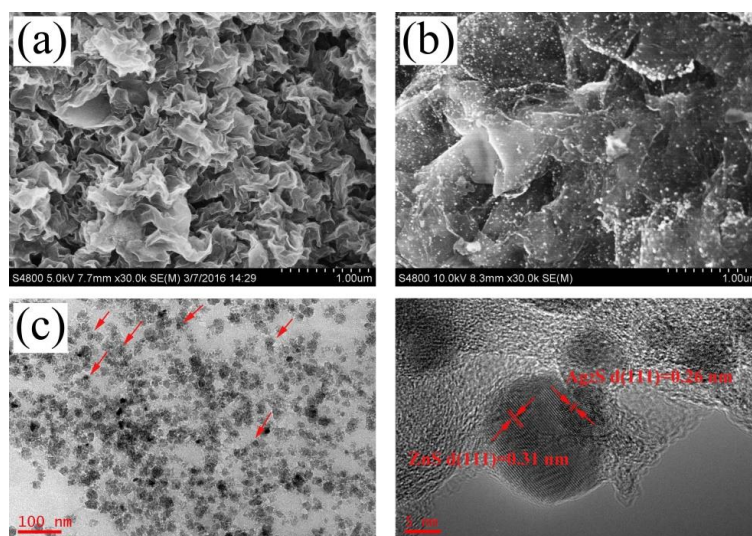
Fig.3. (a) SEM of graphene, (b) SEM. (c) TEM. (d) HRTEM of G-ZnS/Ag$_2$S-2 QD

The morphologies of the as-prepared products were determined with SEM, TEM, and HRTEM. As shown in Fig. 3a, the free-standing two-dimensional GO sheets were crumpled and had a flat structure. The SEM image in Fig. 3b shows a panoramic view of the ZnS/Ag$_2$S quantum dots' morphologies. The quantum dots were densely packed and uniformly anchored on the surfaces of the large graphene sheets. As shown in the TEM image, the nanoparticles about 15 nm in size, and each particle contained some dark regions (marked with an arrow), suggesting the presence of a nanoheterojunction from the ion-exchange reaction. The HRTEM image of G-ZnS/Ag$_2$S-2 QD revealed that the spherical nanoparticles possessed d-spacings of 0.31 nm, corresponding to the (111) plane of ZnS, and 0.26 nm, corresponding to the (111) plane of Ag$_2$S. These results revealed the simultaneous presence of crystalline ZnS and Ag$_2$S.
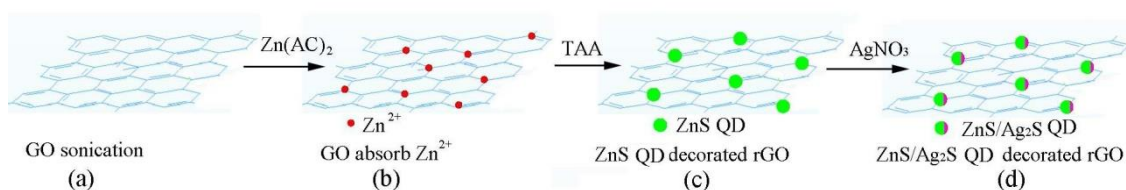
Scheme 1. Proposed scheme of the fabricated processes of G-ZnS/Ag$_2$S QD.

A possible mechanism for the formation of these nanostructures is depicted in Scheme 1. Because of surface-terminated oxygen-containing functional groups such as –OH and –COOH [17], a yellow suspension with uniformly disperse GO was obtained (Scheme 1a). After the addition of Zn(AC)$_2$, oxygen-containing functional groups on GO with a negative surface charge easily adsorbed Zn^{2+} via electrostatic interactions (Scheme 1b) [18]. TAA was added, acting as a sulfur donor and a reducing agent [19]. This led to the reduction of GO and the formation of ZnS quantum dots. Finally, using the G-ZnS QD as a precursor, graphene loaded-ZnS/Ag$_2$S quantum dot heteronanostructures were obtained through a cation-exchange process [20].
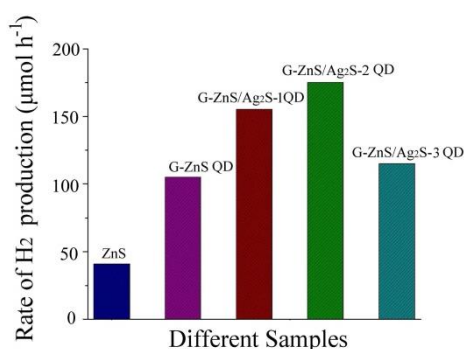
Fig. 4 Photocatalytic H₂ production activities of the samples.

Fig. 4 shows the performances of the nanostructures for photocatalytic H_2 generation while they were irradiated with a 300 W xenon lamp. Na_2S and Na_2SO_3 were added as sacrificial reagents to consume photogenerated holes on the photocatalyst's surface. G-ZnS QD exhibited a higher H_2 production rate (106.3 μmol h^{-1}) than that of ZnS (37.5 μmol h^{-1}). This was attributed to the formation of small nanoparticles and the increased efficiency of interfacial charge transfer in the G-ZnS QD nanocomposites. After the cation-exchange reaction, the G-ZnS/Ag_2S QD system had an improved H_2 generation rate. The H_2 production rates were as high as 115.6 μmol h^{-1}, 175.7 μmol h^{-1}, and 115.6 μmol h^{-1} for the G-ZnS/Ag_2S-1 QD, G-ZnS/Ag_2S-2 QD, and G-ZnS/Ag_2S-3 QD samples, respectively. Enhancements were achieved by the Ag_2S co-catalyst in the nanocomposites, and G-ZnS/Ag_2S-2 QD had the highest H_2 production activity.
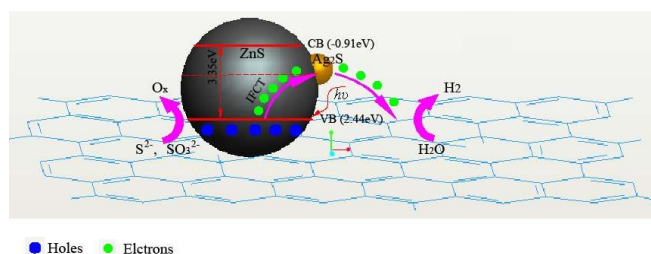
*Scheme 2. Schematic illustration for the charge transfer and separation in the G-ZnS/Ag₂S QD system.*

The high activity for visible light-driven H_2 production of G-ZnS/Ag_2S QD is explained in Scheme 2. Under irradiation by visible light, ZnS quantum dots are not excited because of their wide band gap [21]. After the formation of heteronanostructures containing ZnS quantum dots and Ag_2S, light was absorbed from 350 nm to 450 nm, initiating photoinduced interfacial charge transfer from the valence band of the ZnS quantum dots to Ag_2S [6]. Ag_2S acted as an electron collector. Because the quantum dot heteronanostructures were anchored onto the surface of the graphene, the photogenerated electrons in Ag_2S were directly transferred to graphene, effectively decreasing hole-electron recombination [22]. These electrons then reduced protons to produce H_2 molecules. Meanwhile, the holes remaining in the ZnS quantum dots were consumed by the sacrificial reagents (S^{2-} and SO_3^{2-}) [21].

The possible charge transfers are proposed as the following steps:

(1)Visible light irradiations induce interfacial charge transfer from the VB of ZnS to Ag_2S.

$$ZnS/Ag_2S + h\upsilon \rightarrow ZnS(h^+)/Ag_2S(e^-)$$
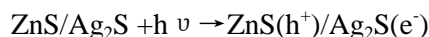
(2) Because of the interaction between ZnS/Ag_2S and graphene, the excited electrons can transfer to graphene.

$$ZnS(h^+)/(Ag_2S) + graphene \rightarrow ZnS(h^+)/Ag_2S + graphene(e^-)$$
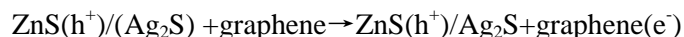
(3) The excited electrons transfer from graphene to H^+.

$$Graphene\ (e^-) + 2H^+ \rightarrow graphene + H_2$$

4. Conclusions

Graphene loaded-ZnS/Ag_2S quantum dot heterostructures were prepared via ion-exchange reactions between preformed graphene-ZnS quantum dots and $AgNO_3$. The graphene-ZnS/Ag_2S quantum dot heteronanocomposites exhibited high photocatalytic activities for H_2 production. Irradiation by visible light was found to initiate photoinduced interfacial charge transfer from the valence band of the ZnS quantum dots to Ag_2S. These electrons were then rapidly transferred from the quantum dots to the graphene. This work demonstrates a generalizable approach to using graphene-based materials for energy conversion.

References

[1] Q.J. Xiang, J.G. Yu, J. Phys. Chem. Lett. **4,** 753 (2013).
[2] Y. Zhong, Q. Wang, Y. He, et al. Anal. Methods **7,** 7874 (2015).
[3] G. Wang, B.B. Huang, Z.J. Li, et al. Nature **5,** 1 (2015).
[4] Y. Hong, J. Zhang, F. Huang, et al. J. Mater. Chem. A **3,** 13913 (2015).
[5] G. Murugadoss, R. Jayavel, M.R. Kumar, et al. Appl. Nanosci. **6**(4), 503 (2016).
[6] X. Zhang, X. Liu, L. Zhang, et al. J Alloy Compd. **655**(15), 38 (2016).
[7] DA Reddy, R Ma, MY Choi, et al. Appl. Surf. Sci. **324,** 725 (2015).
[8] C.C. Wang, Y.C. Hsueh, C.Y. Su, et al. Nanotechnology, **26**(25), 254002 (2015).
[9] H.R Rajabi, M Farsi. J Mol. Catal. A-Chem. **399,** 53 (2015).
[10] S. Pradeep, S. Raghuram, M Chaudhury, et al. J Nanoci. Nanotechno., **17**(2) 1125 (2017).
[11] S. Bai, X.P. Shen. RSC Advances, **2,** 64 (2012).
[12] S.D. Jiang, G. Tang, Y.F. Ma, et al. Mater. Chem. Phys. **151**(1), 34 (2015).
[13] G.Q. Luo, X.J. Jiang, M.J. Li, et al. ACS Appl. Mater. Interfaces **5,** 2161 (2013).
[14] B. Zeng, X. Chen. Dig. J Nanomater. Bio., **11**(2), 559 (2016).
[15] B. Zeng, H. Long. NANO **9**(8), 1450097 (2014).
[16] Md. Selim Arif Sher Shah, A. Reum Park, K. Zhang, et al. ACS Appl. Mater. Interfaces.

4, 3893 (2012).

[17] G.M. Wang, Y.C. Ling, F. Qian, et al. J Power Sources. **196,** 5209 (2011).

[18] B. Zeng, W. Zeng. J Nanomater. Bio. **11**(4), 1105 (2016).

[19] H.T. Hu, X.B. Wang, F.M. Liu, et al. Synth. Met. **161,** 404 (2011).

[20] S. Yue, B.W. Wei, X.D. Guo, et al. Catal. Commun. **76,** 37 (2016).

[21] J. Zhang, J.G. Yu, Y.M. Zhang, et al. Nano Lett. **11,** 4774 (2011).

[22] B. Zeng, W.J. Zeng. Nano **12**(1), 1750005 (2017).